Cellular and Molecular Life Sciences (2023) 80:236
https://doi.org/10.1007/s00018-023-04893-7

ORIGINAL ARTICLE

An impaired splicing program underlies differentiation defects in *hSOD1*^{G93A} neural progenitor cells

Veronica Verdile[1,2] · Veronica Riccioni[2] · Marika Guerra[3] · Gabriele Ferrante[2] · Claudio Sette[3,4] · Cristiana Valle[2,5] · Alberto Ferri[2,5] · Maria Paola Paronetto[1,2]

Received: 7 March 2023 / Revised: 17 July 2023 / Accepted: 19 July 2023 / Published online: 31 July 2023

Abstract

Amyotrophic lateral sclerosis (ALS) is an adult devastating neurodegenerative disease characterized by the loss of upper and lower motor neurons (MNs), resulting in progressive paralysis and death. Genetic animal models of ALS have highlighted dysregulation of synaptic structure and function as a pathogenic feature of ALS-onset and progression. Alternative pre-mRNA splicing (AS), which allows expansion of the coding power of genomes by generating multiple transcript isoforms from each gene, is widely associated with synapse formation and functional specification. Deciphering the link between aberrant splicing regulation and pathogenic features of ALS could pave the ground for novel therapeutic opportunities. Herein, we found that neural progenitor cells (NPCs) derived from the *hSOD1*^{G93A} mouse model of ALS displayed increased proliferation and propensity to differentiate into neurons. In parallel, *hSOD1*^{G93A} NPCs showed impaired splicing patterns in synaptic genes, which could contribute to the observed phenotype. Remarkably, master splicing regulators of the switch from stemness to neural differentiation are de-regulated in *hSOD1*^{G93A} NPCs, thus impacting the differentiation program. Our data indicate that *hSOD1*^{G93A} mutation impacts on neurogenesis by increasing the NPC pool in the developing mouse cortex and affecting their intrinsic properties, through the establishment of a specific splicing program.

Keywords ALS · Alternative splicing · Neural progenitor cells

Introduction

Amyotrophic lateral sclerosis (ALS), also known as Lou Gehrig's disease, is a devastating neurodegenerative disease. The clinical symptoms typically develop between 50 and 70 years. Although most forms are sporadic, familiarity is observed in 10% of the patients [24]. ALS is characterized by muscle wasting due to degeneration of both upper motor neurons (MNs), with their corticospinal axon tracts (Lateral Sclerosis) in the motor cortex, and lower MNs, with their axons in anterior horn of the spinal cord. The progressive loss of MNs causes gradual weakness and paralysis, leading to respiratory failure and death, usually within 3–5 years from diagnosis [24, 50].

The first gene associated with ALS in 1993 was the *Cu2 + /Zn2 + superoxide dismutase 1* (*SOD1*), encoding the free-radical scavenger SOD1 enzyme [43]. Meta-analysis showed that pathogenic *SOD1* variants account for approximately 15–30% of familiar ALS (fALS) and 1–3% of sporadic ALS (sALS) cases [70]. Over 185 disease associated mutations in the *SOD1* gene have been identified, thus leading to variability in the phenotype, duration and severity of the disease [67]. Animal models carrying mutations in human *SOD1* recapitulate many features of ALS, such as oxidative stress, mitochondrial dysfunction, glutamate excitotoxicity, protein aggregation, neuroinflammation and aberrant axonal transport [50].

✉ Maria Paola Paronetto
mariapaola.paronetto@uniroma4.it

1 Department of Movement, Human and Health Sciences, University of Rome "Foro Italico", Piazza Lauro de Bosis 6, 00135 Rome, Italy

2 Laboratory of Molecular and Cellular Neurobiology and of Neurochemistry, Fondazione Santa Lucia IRCCS, Via del Fosso di Fiorano, 64, 00143 Rome, Italy

3 Section of Human Anatomy, Department of Neuroscience, Università Cattolica del Sacro Cuore, 00168 Rome, Italy

4 Fondazione Policlinico Agostino Gemelli IRCCS, 00168 Rome, Italy

5 Institute of Translational Pharmacology (IFT), Consiglio Nazionale delle Ricerche (CNR), 00133 Rome, Italy

Thus, ALS appears as a multifactorial disease, with MN death occurring as the result of a combination of defects in multiple cellular mechanisms [50].

Embryonic neurogenesis represents a complex biological process orchestrating the amplification of the pool of neural progenitor cells (NPCs) with the differentiation and migration of post-mitotic neurons in the developing brain. In the mouse, neurogenesis occurs between the 10th day of embryonal life (E10) and birth [35]. Postnatal neurogenesis continues in specialized areas [28], including the subventricular zone (SVZ) of lateral ventricles [6] and the sub-granular zone of the dentate gyrus in the hippocampus [28]. At first, neuroepithelial cells divide both symmetrically, to generate self-renewing stem cells, and asymmetrically, to give rise to intermediate progenitor cells [38, 49]. Intermediate progenitor cells display a limited mitotic potential and differentiate in post-mitotic neurons, populating the basal compartment of the developing cortex (cortical layer). This developmental process is tightly regulated and allows the correct stratification of the cortex. To accomplish this elaborated program, gene expression networks are finely delineated, allowing coordinated expression in time and space of specific proteins and RNA isoforms [40].

Alternative pre-mRNA splicing (AS) is one of the major mechanisms of gene expression regulation in eukaryotic cells. By generating several mature mRNA isoforms from the same pre-mRNA [36], AS expands the genomic coding capacity and the proteomic diversity in eukaryotic cells [36, 57]. Proteins encoded by alternatively spliced transcripts can show differences in their subcellular localization, post-translational modifications and/or functions [7]. In some cases, AS does not cause differences in the protein sequence, but rather it affects the stability of the alternative transcripts, determining when a specific protein isoform is available to the cell. Indeed, AS can even generate premature termination codons (PTCs), which are targets of nonsense-mediated mRNA decay (NMD) [4, 17, 25, 37, 69].

Numerous studies have reiterated the critical and fundamental role of AS in the mammalian nervous system, by enhancing cell-identity acquisition, cell growth and differentiation [4, 8, 45, 48, 68]. AS contributes to the establishment and/or maintenance of the functional complexity of the brain by affecting important processes such as axon guidance, synapse formation, and regulation of membrane physiology [7, 40, 58, 62]. High-throughput RNA-sequencing analyses revealed that brain displays the most complex and dynamic AS network, leading to expression of specific protein isoforms [11, 26, 64, 65]. Splicing abnormalities and defects in the spliceosome machinery, or in the accessory RNA-binding proteins (RBPs), influence the pathogenesis of human diseases, including ALS, and can represent a key factor driving disease severity but also vulnerability [60].

Increasing evidence suggests that MNs carrying SOD1-ALS mutations show alterations already at pre-symptomatic stages [1, 9, 18, 30, 59]. Accordingly, spine loss in the motor cortex of *hSOD1*^{G93A} mouse model occurs before the onset [1, 19]. Deciphering the link between aberrant splicing regulation and pathogenic features could pave the ground for novel therapeutic approaches to ALS. Herein, we found that NPCs derived from *hSOD1*^{G93A} mice display strongly increased proliferation and propensity to differentiate into neurons. Furthermore, these effects were robustly attenuated at 7 days of differentiation. In parallel, *hSOD1*^{G93A} NPCs showed impaired splicing patterns that could contribute, at least in part, to the observed phenotype. These findings indicate that the *hSOD1*^{G93A} mutation impacts on neurogenesis by increasing the NPC pool in the developing mouse cortex and affecting the intrinsic properties of these cells.

Methods

Neural progenitor cells isolation and culture

Neural progenitor cells (NPCs) were isolated from C57/BL6 SOD1G93A and wild-type (WT) (Charles River Laboratories, Sulzfeld, Germany) embryonic mouse cortex at embryonic day 13.5 (E13.5), following the Institutional guidelines of the Fondazione Santa Lucia and the approval of the local Ethical Committee. After olfactory bulbs, ganglionic eminences and meninges removal, embryonic cortices were isolated, mechanically disaggregated and centrifugated, the pellet was resuspended in neurosphere medium consisting of DMEM-F12 (1:1) with GlutaMAX™, B27 (1 ml/50 ml, Thermo Fisher Scientific), penicillin (100 U/ml), streptomycin (100 mg/ml) and supplemented with epidermal growth factor (EGF, 20 ng/ml, Peprotech, United Kingdom) basic fibroblast growth factor (bFGF, 20 ng/ml, Peprotech) and heparin (0.5 U/ml, Sigma-Aldrich). The cells were incubated in a humidified atmosphere with 6% CO_2 at 37 °C. For clonal analysis, 2500 NSCs were plated in 35-mm wells. After 3, 5 and 7 days of culture in proliferating conditions, neurospheres number was evaluated and NPC clonogenicity was calculated as ratio between plated cells and neurospheres formed, expressed as percentage. For the differentiation studies, dishes were coated with poly-lysine (Sigma-Aldrich) in PBS for 20 min under UV irradiation. After three washes in PBS, cells were plated in neurosphere medium containing 1% FBS and incubated in a humified atmosphere with 6% CO_2 at 37 °C until 7 days. For transfection, cells were transfected using the NEPA21 (Nepagene) electroporator, using control, *Rbfox1* or *Ptbp1* oligonucleotides (SASI_Mm01_00150775 and SASI_Mm02_00292552). Briefly, 1.5 million cells for each point were transfected in Optimem medium, using 300 nM of siRNA. Settings for the

Poring Pulse: 100 V, length 5 ms, interval 50 ms, no. 2, d.rate 10%, polarity +. Settings for the Transfer Pulse: 20 V, length 50 ms, interval 50 ms, no. 5, d.rate 40%, polarity ±. RT-qPCR was performed to verify *Rbfox1* and *Ptbp1* downregulation, using *Tbp* as housekeeping gene.

Cell cultures and transfections

Mouse N2A cells (ATCC) were maintained in Dulbecco's Modified Eagle Medium (DMEM, GIBCO—Thermo Fisher Scientific, Waltham, USA, Massachusetts) with GlutaMAX™, supplemented with 10% fetal bovine serum (FBS), penicillin (100 U/ml) and streptomycin (100 mg/ml) (all from GIBCO). For differentiation studies, cells were plated in DMEM with GlutaMAX™, supplemented with 0.5% FBS, penicillin (100 U/ml) and streptomycin (100 mg/ml) for 6 days. Transfection of N2A cell line was performed using RNAimax reagent (Thermo Fisher Scientific) according to manufacture's instructions. Briefly, 50,000 N2A cells were subjected to double pulse of reverse-transfection using 2 µl of Lipofectamine RNAiMAX, and cells were collected 24 h after the last pulse of transfection. N2A cells were transfected with control siRNA and siRNA for *Rbfox1* and *Ptbp1* (Sigma-Aldrich, St Louis, MO, USA, (SASI_Mm01_00150775 and SASI_Mm02_00292552)) at the final concentration of 25 nM. RT-qPCR was performed to verify *Rbfox1* and *Ptbp1* downregulation, using *Tbp* as housekeeping gene.

NSC-34 motor neurons are a mouse neural hybrid cell line arising by the fusion of motor neuron-enriched embryonic mouse spinal cord neurons with mouse neuroblastoma cells [12]. NSC-34 cells expressing either WT or mutant human SOD1G93A DNA [16] were cultured in DMEM/F12 medium supplemented with 10% FBS, penicillin (100 U/ml) and streptomycin (100 mg/ml) (all from GIBCO). *Rbfox1* and *Ptbp1* knockdown was performed as described above. For induction of differentiation into the motor neuron-like phenotype, NSC-34 cells were plated in DMEM/F12 supplemented with 0.5% FBS, penicillin (100 U/ml), streptomycin (100 mg/ml) and 1% modified Eagle's medium non-essential amino acids (NEAA, 100X Gibco), for 3 days.

Embryo genotyping

Tails were digested with 500 µl of Tail buffer each (Tris–HCL pH 8 0.5 M, 250 µl Tween, 2.5 ml NP40 10%) supplemented with proteinase K (100X) and left overnight at 56 °C. The day after the proteinase K was inactivated at 75 °C for 20 min. For the genotyping is prepared a mix composed of 5X buffer, 10 µM primers (forward and reverse), 25 mM dNTPs, the GoTaq polymerase (5 u/µl), to this is added 1 µl of tail DNA (diluted 1:100) previously digested. The samples were run on an agarose gel, with the presence also of a positive (+hSOD1) and a negative (-hSOD1) control.

Isolation of RNA and conventional and quantitative PCR

Total RNA was isolated using TRIzol Reagent (Thermo Fisher Scientific) according to the manufacturer's instructions. RNA was subjected to DNAse digestion (Qiagen) and the first-strand cDNA was obtained from 1 µg of RNA using random primers and M-MLV Reverse Transcriptase (Promega, Madison, WI, USA), following the manufacturer's instructions. Synthesized cDNA was used for conventional PCR (GoTaq G2, Promega) and quantitative PCR (SYBR Green Master Mix for Light-Cycler 480, Roche, Basel, Germany), according to manufacturer's instructions. For splicing assay experiments, conventional PCR analysis was performed after 35 cycles. The ratio between isoforms related to included and skipped exons was calculated from densitometric analysis by ImageJ software. Primers used for qPCR and PCR analyses are listed in Supplementary Table 1. The comparative cycle threshold (ΔCt) method was used to analyze the absolute expression levels using *Tbp* as control.

Immunofluorescence analysis

For immunofluorescence analysis, NPCs cultured in differentiating condition were fixed with 4% paraformaldehyde (Sigma-Aldrich) and permeabilized with 0.1% Triton X-100 in PBS, supplemented with 1% BSA. Primary antibodies (2 h at RT): with mouse anti-β-III-tubulin (1:400, T8578, Sigma-Aldrich), mouse anti-GFAP (1:400, NBP1-05197, Novusbio), rabbit anti-MBP (1:400, 78896, Cell Signaling). After PBS washes, cells were incubated with Cy2-conjugated goat anti-mouse IgG (1:500, Alexa, Life Technologies), Cy3-conjugated goat anti-rabbit IgG (1:500, Alexa, Life Technologies), secondary antibodies (Jackson ImmunoResearch) for 1 h at RT and with DAPI (Invitrogen, United Kingdom) for 15 min. 10 µl of Mowiol was used to close the slides. Samples were then viewed and photographed using confocal laser-scanning microscope (Zeiss, LSM700, Germany). Data are represented as percentage of positive cells/total cells (evaluated by the number of total nuclei). Neurite length was calculated with the ImageJ software, as previously described [39]. Briefly, analysis was performed by manual tracing of neurite length using neurite tracer and counter plugins in the ImageJ software. Images of three fields per well were taken and the neurite length was calculated from the base of the soma to the end of the neurite. Data were obtained from three independent experiments.

External dataset and bioinformatic analysis

Neural progenitor cells (NPCs) and neurons purified from E15.5 cortical cells were downloaded from the Gene Expression Omnibus with accession GSE96950 (Liu J et al., 2018). The RNA-seq data of NPCs and neurons were re-analyzed using the cutoff of $P \leq 0.05$, and threshold 1.5 for gene expression (Supplementary Table 2) and splicing index fold change (Supplementary Tables 3, 4). For different alternative splicing events, gene ontology analysis was performed using EnrichR bioinformatic tool [29] to identify the most enriched Gene Ontology (GO) categories and pathways across the down- and upregulated events.

Bioinformatic analysis

Gene expression and AS analysis of transcriptomic data GSE96950 (Liu J et al., 2018) were performed by GenoSplice technology (http://www.genosplice.com). Analysis at gene expression and splicing levels were performed as previously described using Mouse FAST DB v2013_2 annotations [15]. For analysis of cis-regulatory sequences and elements of regulated cassette exons, genes expressed according to the GSE96950 RNA-seq data, but not regulated neither at the gene or exon/pattern level, were considered as reference genes. Search for enriched motifs within regulated cassette exons and their comparison with the compendium of RNA-binding motif from [41] were performed using DREME and Tomtom Motif comparison tools from the MEME Suite Collection (Supplementary Tables 5, 6) [23]. Analysis for enriched GO functional clusters among AS-regulated genes was performed as previously described [61].

Statistical analysis

Independent experiments were performed in technical and biological triplicates. The results were expressed as mean value ± standard deviation (SD). Statistical analysis for biological assays was performed using Graphpad Prism software. Student *t* test was used for comparison of two groups and the one-way analysis of variance (ANOVA) was performed to analyze multiple comparisons. The values with $P \leq 0.05$ (*) were considered significant.

Results

hSOD1^{G93A} neural progenitor cells display higher initial proliferative potential

The number of neurons produced during neurogenesis is balanced by the initial pool of NPCs and their progressive switch from self-renewing to neurogenic divisions [38, 49]. To evaluate whether the *hSOD1*^{G93A} background affected NPC properties, these cells were isolated from the embryonic cortex at E13.5 days from either *hSOD1*^{G93A} transgenic or wild-type mice (Fig. 1A) and NPC-derived neurospheres were counted at different time points of culture. As shown in Fig. 1B, *hSOD1*^{G93A} NPCs displayed a significantly increased ability to form neurospheres at day 3 and day 5, which then declined to the levels of wild-type NPCs at day 7. These data suggest an initial higher clonogenic potential of *hSOD1*^{G93A} NPCs. Visual inspection of the neurospheres obtained indicated that those deriving from *hSOD1*^{G93A} NPCs were larger than their wild-type counterpart (Fig. 1C). These results suggest that expression of the *hSOD1*^{G93A} enhances the early stemness potential and proliferative activity of NPCs, yielding to an initial amplification of the NPC pool in vitro, which is not supported at later time points.

hSOD1^{G93A} neural progenitor cells early differentiate in neurons

Embryonic NPCs can either self-renew or enter in a committed state, which ultimately result in differentiation into post-mitotic neurons [38, 49]. To evaluate their potential to self-renew and differentiate, *hSOD1*^{G93A} NPCs were seeded on plates coated with poly-lysine, in the presence of 1% of FBS (Fig. 2A). RT-qPCR and immunofluorescence analyses were performed to evaluate markers of neuronal differentiation at different time points. RT-qPCR analysis before differentiation was started revealed that the stemness markers *Nestin*, *Sox2* and *Pax6* were significantly more expressed in *hSOD1*^{G93A} NPCs with respect to wild-type NPCs (Fig. 2B–D).

Next, we evaluated differentiation of NPCs by immunofluorescence analysis of markers of neurons (β-III-tubulin), oligodendrocytes (MBP) and astrocytes (GFAP) at day 3 and 7 of differentiation. Remarkably, we observed an altered time course of neuron differentiation in NPCs h*SOD1*^{G93A} cultures. After 3 days of differentiation, β-III-tubulin-positive cells were significantly increased with respect to wild-type cultures, but this effect was inverted at day 7, when *hSOD1*^{G93A} neurons declined and were significantly fewer that those generated by wild-type NPCs (Fig. 3A, C). Furthermore, analysis of neurite length after 3 days of differentiation showed that *hSOD1*^{G93A} neurons displayed very long neurites (average length > 100 µm) in comparison with wild-type neurons. However, this difference was abolished after 7 days of differentiation (Fig. 3D). A similar trend of altered differentiation was also observed for oligodendrocytes (MBP-positive cells) and astrocytes (GFAP-positive cells), albeit the increase at day 3 was not statistically significant (Fig. 3A, C). These results highlight changes in the clonogenic and differentiation potential of NPCs derived from the *hSOD1*^{G93A} transgenic mouse model.

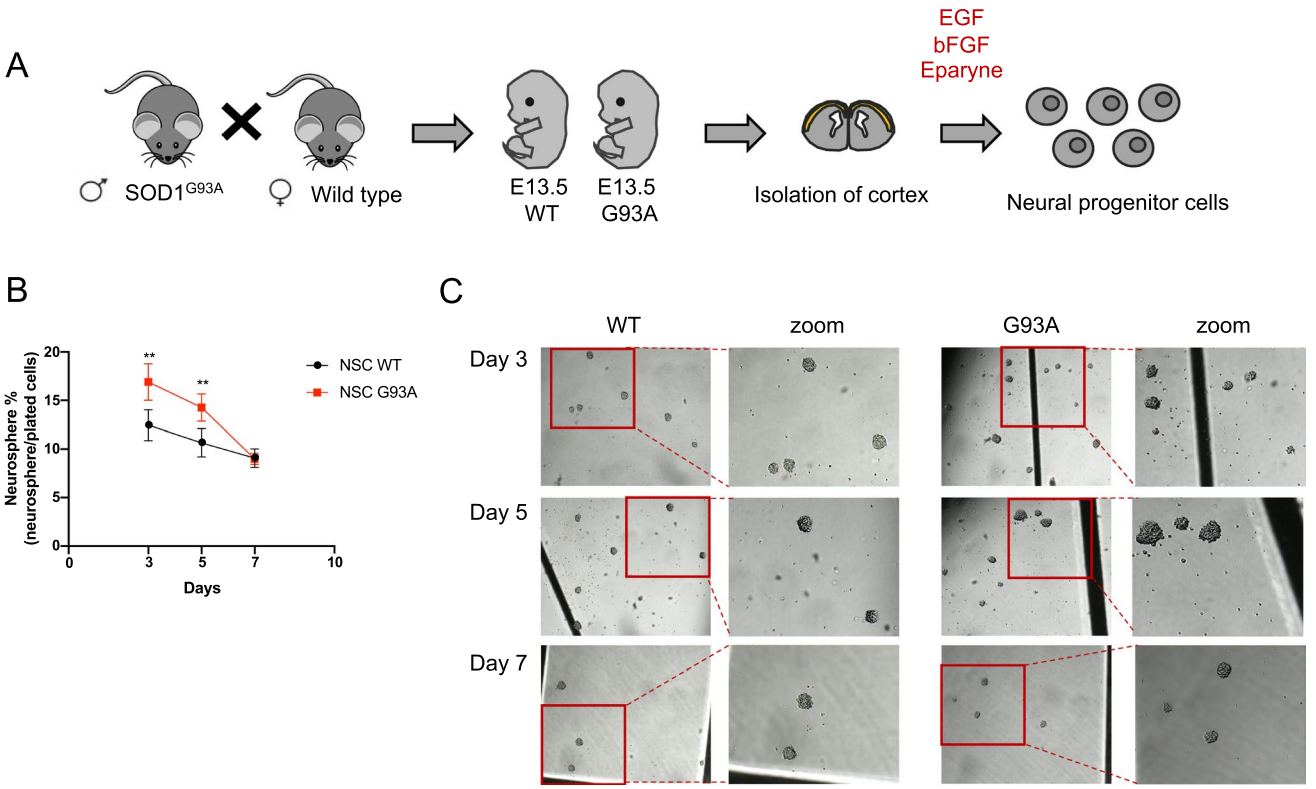

Fig. 1 *hSOD1*^{G93A} neural progenitor cells (NPCs) display an initial boost of clonogenicity. **A** Representative scheme of the isolation and culture of the neural progenitor cells (NPCs). **B** Clonogenic assay of NPC *SOD1*^{WT} and *hSOD1*^{G93A}. Clonogenicity was expressed as the percentage of the neurospheres obtained from the plated NSC at each passage ($n=4$; mean ± SD; $^{**}P \leq 0.01$). **C** Representative bright field images of neurospheres obtained from NPCs *hSOD1*^{WT} and *hSOD1*^{G93A} cultured in proliferating condition for 3, 5 and 7 days

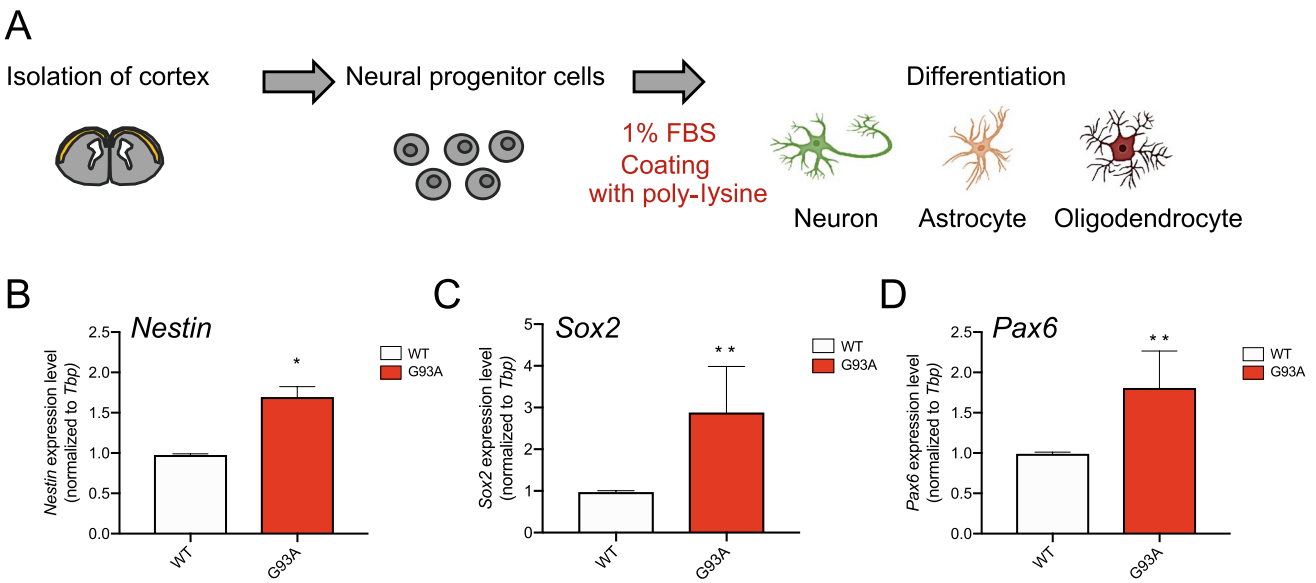

Fig. 2 *hSOD1*^{G93A} impacts stemness markers in NPCs. **A** Representative scheme of experimental design to differentiate NPCs. **B–D** The graphs show the results of RT-qPCR analysis of the stemness markers *Nestin, Sox2* and *Pax6* in proliferating (day 0) NPCs *hSOD1*^{WT} and *hSOD1*^{G93A}, normalized for levels of the housekeeping gene *Tbp.* Values are the mean ± SD of three independent experiments, considering the *hSOD1*^{WT} condition as 1. Statistical analysis was performed by Student's *t* test, *P* values: $^{*}P \leq 0.05$; $^{***}P \leq 0.001$

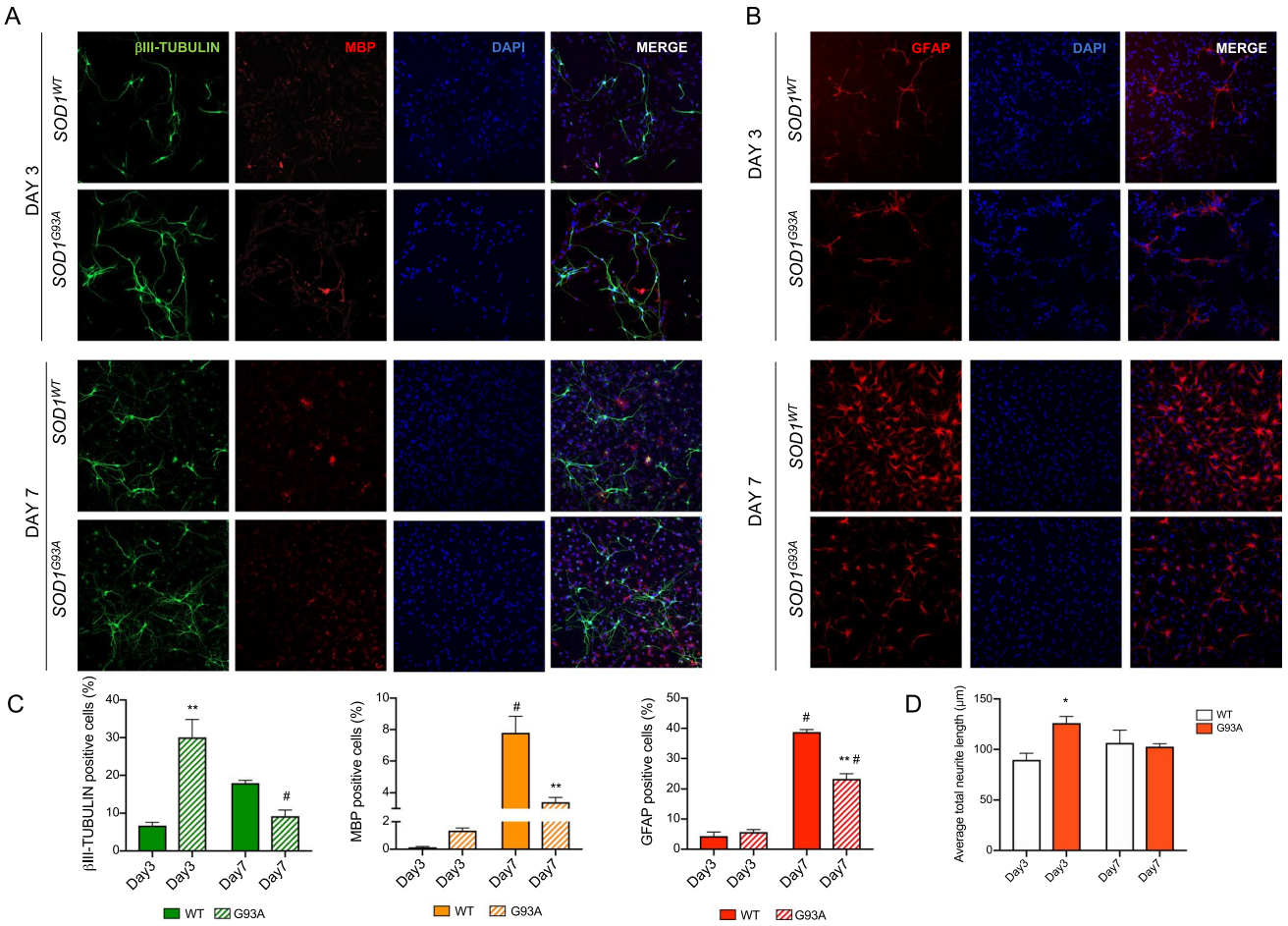

Fig. 3 *hSOD1*^{G93A} neural progenitor cells display early differentiation. **A–B** Representative images of *hSOD1*^{G93A} and *hSOD1*^{WT} NPCs, cultured for 3 and 7 days in differentiating condition. Scale bar = 50 μm. **A** Cells were stained with anti-βIII tubulin (green), anti-MBP (red), and DAPI (blue). **B** Cells were stained with anti-GFAP (red) and DAPI (blue). **C** Bar graph representing the percentage of βIII-tubulin, MBP- and GFAP-positive cells. Data represent mean ± SD of 3 independent experiments. Statistical analysis was performed by one-way ANOVA, with P value ≤ 0.05, and with Bonferroni post hoc test (P value ≤ 0.05; *comparison within the group, # comparison between groups). **D** *hSOD1*^{G93A} affects neuronal differentiation in NPCs. Bar graph represents the average of total neurite length per cell (μm). P values were determined by Student's t test $^{*}P \leq 0.05$ ($n = 3$; mean ± SD)

Our data indicate that the *hSOD1*^{G93A} background promotes a transient increase in stem-like features and proliferation of NPCs, but their differentiation properties result impaired.

Alternative splicing is affected in *hSOD1*^{G93A} neural progenitor cells

Neuronal differentiation is orchestrated by profound changes in gene expression and AS. Analysis of the splicing patterns that are differentially regulated between NPCs and neurons (GSE96950; Supplementary Tables 2, 3) identified 416 splicing events, with exon cassette as the most represented type of event (Fig. 4A, B). Gene ontology analysis using the *Enrichr* database highlighted morphogenetic changes of neurons and microtubule polymerization/depolymerization as the most enriched biological functions related to the splicing-regulated genes (Fig. 4C) while Reactome pathway analysis indicated the protein–protein interaction at synapses as the most enriched pathway (Fig. 4D).

Given the pivotal role played by AS in synapse formation and plasticity [21], we asked whether splicing changes in genes related to neuronal differentiation were impaired in NPCs derived from h*SOD1*^{G93A} embryos. To this end, total RNA was extracted and purified from wild-type and *SOD1*^{G93A} NPCs at day 0 and day 7 of differentiation and AS of genes encoding components of the synaptic compartment that are necessary for the maintenance of the synapse structure and function was investigated.

The *Add1* gene encodes a membrane-cytoskeleton-associated protein that promotes the assembly of the spectrin–actin network and the correct structure and diameter of axons [31, 66]. The *Akap9* gene encodes the A-kinase anchoring

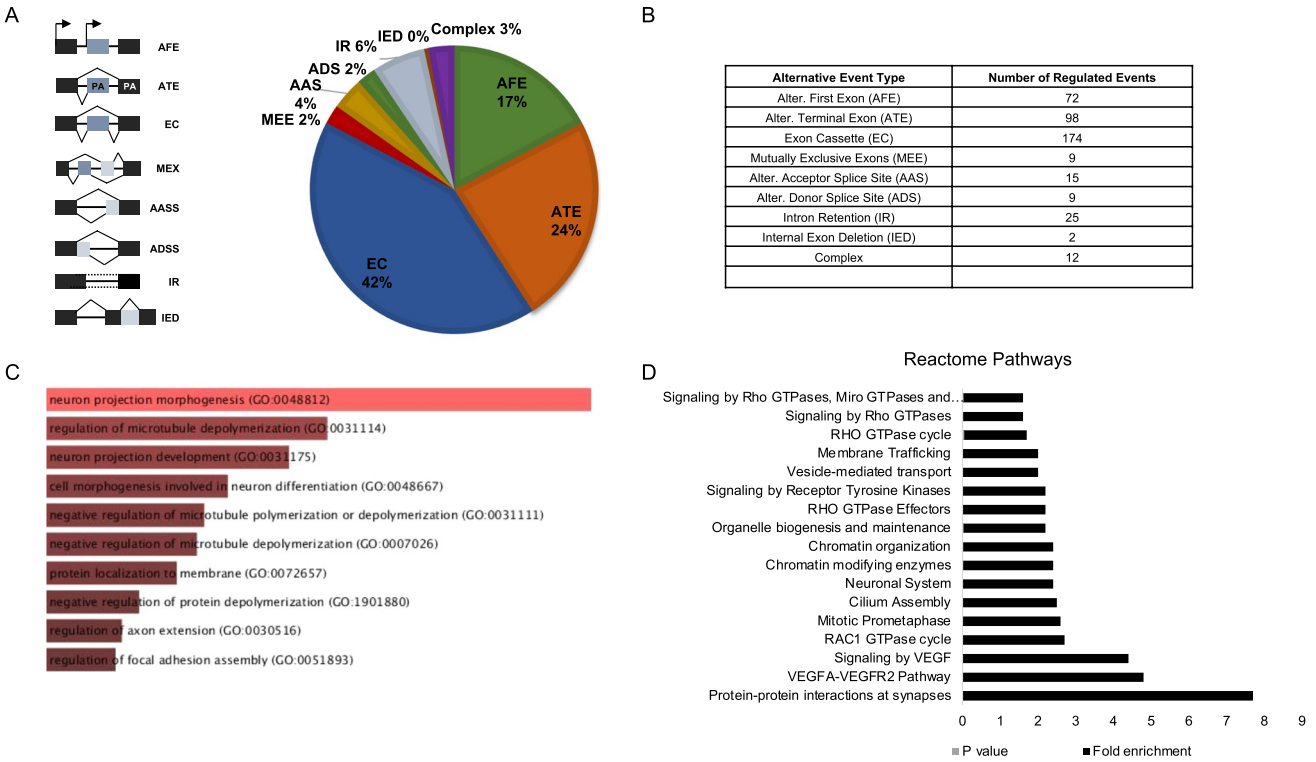

Alternative Event Type	Number of Regulated Events
Alter. First Exon (AFE)	72
Alter. Terminal Exon (ATE)	98
Exon Cassette (EC)	174
Mutually Exclusive Exons (MEE)	9
Alter. Acceptor Splice Site (AAS)	15
Alter. Donor Splice Site (ADS)	9
Intron Retention (IR)	25
Internal Exon Deletion (IED)	2
Complex	12

Fig. 4 Alternative splicing shapes neuronal differentiation. **A** Pie chart representing distribution of regulated splicing events among different splicing patterns in NPCs and neurons obtained by analyzing the GSE96950 dataset. **B** Table representing the type of alternative splicing event and number of regulated events in NPCs vs neurons. **C** Bar graph showing the enrichment score of the gene ontology functional clusters enriched in splicing-regulated genes obtained with the EnrichR tool (https://maayanlab.cloud/Enrichr/). **D** Bar graph represent the enrichment score of Reactome pathways from the splicing-regulated genes

protein (AKAP), which belongs to a large family of structurally diverse scaffolding proteins, specifically enriched in the neuromuscular junction (NMJ) and in the neuronal synapse [33]. Analysis of *Add1* and *Akap9* transcripts revealed a mild but significant reduction in skipping of the alternative exons (15 and 3A, respectively) in the *hSOD1*^{G93A} condition compared to control at day 7 of differentiation (Fig. 5A, B). *Camsap1* gene encodes the Calmodulin-Regulated Spectrin-Associated Protein 1 (CAMSAP1) required for neurite outgrowth and axonogenesis. Mutation in this gene induced overextension of neurites and impaired axon regeneration [14, 34]. The regulated alternative exon encodes a protein domain that facilitates interactions with synaptic membrane proteins [13]. Notably, the inclusion of exon 4A in *Camsap1* was significantly reduced in *hSOD1*^{G93A} NPCs after 7 days of differentiation (Fig. 5C). The *Cask* gene encodes a multidomain scaffolding protein with a role in synaptic transmembrane protein anchoring and ion channel trafficking [2]. Upon differentiation, we observed increased skipping of the alternative exon 10A in *Cask* pre-mRNA in the *hSOD1*^{G93A} (Fig. 5D). Notably, this alternative exon encodes a protein domain that facilitates interactions with synaptic membrane proteins. Analysis of *Mark3* transcripts, encoding the Microtubule Affinity Regulating Kinase 3, showed more inclusion of the alternative exon 3A both at day 0 and day 7 of differentiation in *hSOD1*^{G93A} NPCs compared to control (Fig. 5E). The *Pkt2* gene encodes a non-receptor protein-tyrosine kinase that plays a key role at focal adhesion sites, in promoting spreading, migration, and transmission of anchorage-dependent antiapoptotic signals [46]. PTK2 is subject to autophosphorylation at Tyr-397, a key event for PTK2 function. AS events in *Ptk2* alter the autophosphorylation rate of the encoded protein in neurons; in particular, the isoform showing the inclusion of exon 14B and 15A, and the isoform showing the inclusion of exon 14B, 15A and 14A, display an increased autophosphorylation [10, 52]. Skipping of the alternative exon 15A was favored in NPC *hSOD1*^{G93A} compared to the wild type after 7 days of differentiation (Fig. 5F), thus potentially contributing to lower autophosphorylation of PTK2 protein kinase. Notably, in most of the genes analyzed, we observed a change of AS pattern (i.e., increased inclusion or increased skipping) between day 0 and 7 of differentiation, which was attenuated or abolished in *hSOD1*^{G93A} cells.

These experiments highlight changes in AS of synaptic-related genes in NPCs *hSOD1*^{G93A} at the onset of neuronal

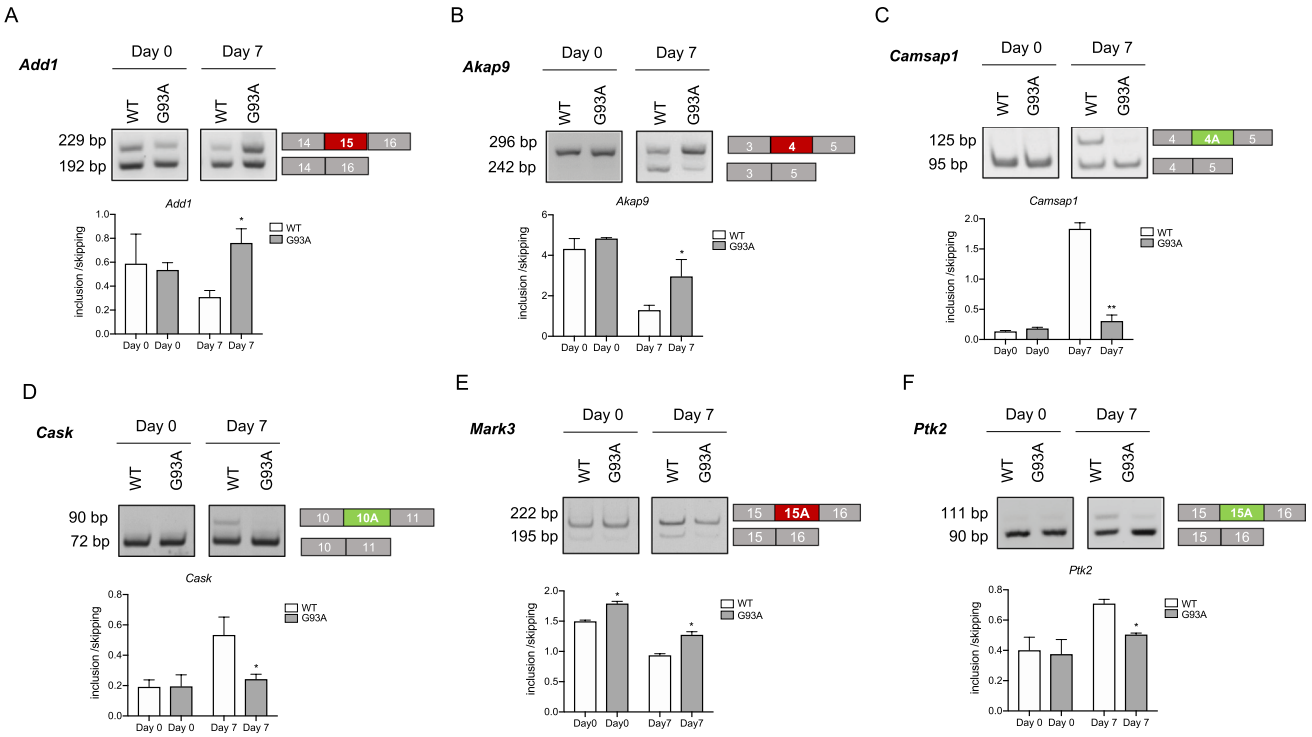

Fig. 5 *hSOD1*^{G93A} mutation modulates alternative splicing of synaptic-related genes in NPCs. **A–F** Representative images of the PCR analyses for the indicated splicing events (*Add1*, *Akap9*, *Camsap1*, *Cask*, *Mark3*, *Ptk2*) differentially regulated between proliferating (day 0) and differentiated (day 7) *hSOD1*^{G93A} and SOD1 ^{WT} NPCs. Schematic representation for each event analyzed is depicted on the right of the representative agarose gel. Red boxes indicate the upregulated exon, green boxes indicate downregulated exon, gray boxes indicate the constitutive exon in *hSOD1*^{G93A} compared with control cells. The graphs show the densitometric analysis of the ratio between isoforms with included and skipped exons. Statistical analysis was performed by one-way ANOVA with Bonferroni post hoc test (*P* value: * < 0.05; *P* value: ** < 0.01)

differentiation and provide support to previous studies reporting alterations in the synapse, at both morphological, physiological and functional levels, in MNs carrying SOD1-ALS mutations [1, 9, 20, 30, 59].

RBFOX1 and PTBP1 motifs are enriched in neuronal-sensitive exons

Analysis of cis-regulatory sequence elements enriched in the regulated cassette exons and their flanking introns identified several consensus motifs, including CUCUC and GCAUG. These motifs correspond to the binding sites of PTBP1 (CUCUC) and RBFOX1 (GCAUG), two splicing factors known to play a pivotal role in the neuronal differentiation program [22, 69]. These motifs were enriched, respectively, in the intron upstream and downstream of upregulated exons (Fig. 6A). In addition, by considering a motif enrichment higher than twofold versus reference and an adjusted *P* value ≤ 0.05, we also identified other regulatory motifs as significantly represented in the proximity of the regulated exons (Fig. 6A and Supplementary Tables 4, 5). Remarkably, during neuronal differentiation PTBP1 and RBFOX1 antagonistically govern the NPC-to-neuron transition by regulating neuron-specific exons [69]. This specific and rigorous regulation is ensured by gene expression changes in the splicing factor network (Fig. 6B, Supplementary Table 6). Indeed, our bioinformatic analysis indicated that, in addition to *Rbfox1* upregulation and *Ptbp1* downregulation, other splicing factors displayed significant changes in their expression profile during neuronal differentiation (Fig. 6B). Although expression of RBPs known to be involved in ALS, such as TDP-43 and FUS, was not modulated during neuronal differentiation, we found that regulatory motifs recognized by these RBPs (FUS: GGGGG, GGTGG, GGCTG, GGCGG, GCGGC; TDP-43: GTGTG, TGTGT) are enriched in neuronal-sensitive exons (Suppl. Tables 4–5). Moreover, comparison of genes displaying neuronal-sensitive exons with those regulated at the splicing level by TDP-43 silencing in NSC-34 motor neuron-like cells [71] or by FUS mutations causing cytoplasmic aggregates [42] revealed a significant overlap (Suppl. Fig. 1).

Next, we asked whether the aberrant splicing changes observed in the differentiating *hSOD1*^{G93A} NPCs could be due to alteration in splicing factor pattern. To answer

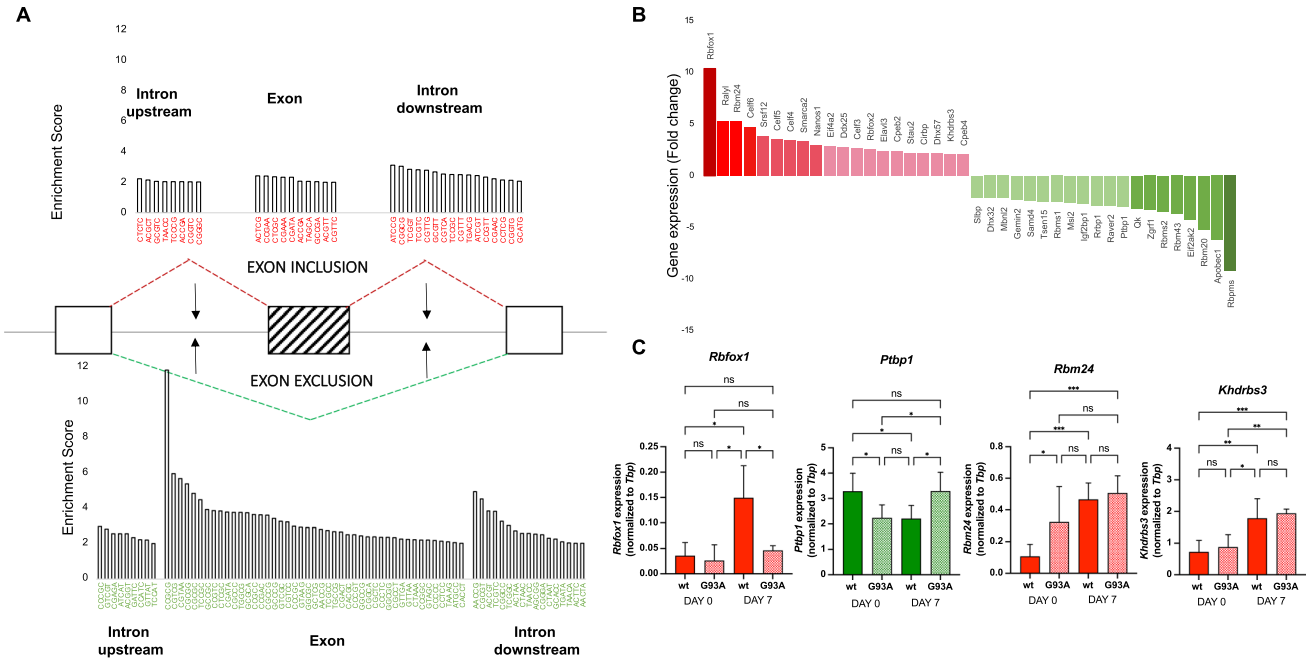

Fig. 6 Specific cis-acting elements feature neuron signature. **A** Schematic representation of predicted RBPs binding cis-acting elements within or nearby (±250 bp in the surrounding introns) neuron-sensitive cassette exons. The scheme also reports pentamer enrichments within regulated exons. For the conserved and enriched pentamers, see also Supplementary Tables 5, 6. **B** Expression profile of RBPs from the transcriptome analysis. Bar graphs represent gene expression fold changes of neurons versus NPCs. In red are represented RBPs upregulated at least 2.0 versus control. In green are represented RBPs downregulated at least 2.0 vs control. See also Supplementary Table 4. **C** The graphs show the results of RT-qPCR analysis of the *Rbfox1*, *Ptbp1*, *Rbm24* and *Khdrbs3* transcripts in proliferating (day 0) and differentiating (day 7) NPCs *hSOD1*^{WT} and *hSOD1*^{G93A} normalized for the expression of *Tbp* housekeeping gene. Values are the mean ± SD of three independent experiments. Statistical analysis was performed by one-way ANOVA with Bonferroni post hoc test. *P* values: $*P \leq 0.05$; $**P \leq 0.01$; $***P \leq 0.001$

this question, RT-qPCR analysis was performed on RNA extracted NPCs at different time points of differentiation. Our analysis confirmed the upregulation of *Rbfox1* and the downregulation of *Ptbp1* transcripts during differentiation of wild-type NPCs. However, no significant differences in *Rbfox1* expression were observed between day 0 and day 7 of differentiation in the *hSOD1*^{G93A} NPCs (Fig. 6C). *Ptbp1* expression also displayed an altered pattern in *hSOD1*^{G93A} NPCs, with a significant reduction at day 0 and an increase at day 7 (Fig. 6C). Moreover, the upregulation of *Rbm24* observed during differentiation of wild-type NPCs was attenuated in the *hSOD1*^{G93A} NPCs, whereas a similar expression pattern was observed for *Khdrsbs3* transcript (Fig. 6C).

Since PTBP1 and RBFOX proteins were shown to play a key role in the NPC-to-neuron transition [69], we sought to investigate them further. Knockdown experiments of both *Ptbp1* and *Rbfox1* transcripts in N2A neuronal cells confirmed the regulation of *Add1*, *Akap9*, *Camsap1*, *Cask* and *Ptk2* splicing by these splicing factors (Suppl. Fig. 2A–H). Remarkably, silencing of *Ptbp1* and *Rbfox1* also affected the clonogenic properties and neuronal differentiation of NPCs, as revealed by the increase in the percentage of proliferating neurospheres at early time points after *Rbfox1* silencing and the decrease in the neuronal markers at 7 days of differentiation in si*Rbfox1* and *siPtbp1* NPCs (Suppl. Fig. 3A–F). Moreover, in NSC-34 motor neuron-like cells, in which expression of SOD1G93A induced β-III-tubulin expression like in NPCs at day 3 of differentiation (Supp. Fig. 4A), silencing of *Ptbp1* recapitulated this effect, whereas silencing of RBFOX1 exerted a milder effect (Supp. Fig. 4B–D). These results suggest that the altered expression pattern of these splicing regulators in the *hSOD1*^{G93A} NPCs contributes to the defects in their clonogenic and differentiation properties.

Discussion

Alterations in synaptic function and morphology accompany in the early phases of ALS [1, 9, 20, 30, 59]. Mouse models of ALS disease greatly helped in the understanding of synaptic failure. For example, embryonic and neonatal *hSOD1*^{G93A} spinal MNs showed elevated hyperexcitability, increased persistent $Na^{(+)}$ and enhanced frequency of spontaneous excitatory and inhibitory transmission [1, 9, 20, 30, 59]. MNs of *SOD1*^{G85R} mouse pups displayed an excessive

elongation and overbranching at early postnatal life [18]. The resulting enlarged dendritic morphology caused dysfunction of the synapses, leading to defective pruning mechanisms [1], probably due to the increased ratio between excitatory and inhibitory synapses, hyperexcitability, and consequent neuronal death [3, 30, 59]. Given these reported findings, we first aimed at evaluating the impact of *hSOD1*^{G93A} mutation on the clonogenicity and differentiating potential of embryonic NPCs. We observed that *hSOD1*^{G93A} NSCs displayed a boost in forming neurospheres at the onset of cell culture in comparison with the wild-type NPCs (Fig. 1). In line with the reported excessive elongation of the MNs at early postnatal life in SOD1^{G93A} pups [18], our data show that after 3 days of in vitro differentiation the main difference between wild-type and *hSOD1*^{G93A} NPCs is the increased neurite length in *hSOD1*^{G93A} cells, that could be due to hyperexcitability and alteration of synaptic input. After 7 days of differentiation, we did not observe differences of neurite length between *hSOD1*^{G93A} and *hSOD1*^{WT}, but rather we noticed a reduced βIII-Tubulin expression in *hSOD1*^{G93A} differentiating NPCs compared to *hSOD1*^{WT}, highlighting defects in the maintenance of the acquired morphology affecting the neuronal function.

NPCs can differentiate into neurons, astrocytes and oligodendrocytes, which are the cellular classes mainly affected in ALS [53, 56]. Regarding glial cells, after 7 days of differentiation, *hSOD1*^{G93A} NPCs showed reduced expression of GFAP, which is a marker of astrocytes, in comparison with wild-type NPCs [49]. The expression of the oligodendrocyte marker MBP [49] was also lower in the *hSOD1*^{G93A} differentiating NPCs. These results indicate an aberrant clonogenicity and differentiating capacity of *hSOD1*^{G93A} NPCs.

Cell-type specific gene expression networks shape the synapse functions and properties. AS regulation also plays a pivotal role in synapse formation and in synaptic plasticity [21]. Splicing regulators orchestrate a dynamic post-transcriptional program supporting cellular diversity and allowing neuronal circuits and a broad range of complex behaviors [5, 57, 65]. Genetic deletion of neuronal RBPs results in severe alterations in AS programs, leading to embryonic lethality and/or neuronal diseases [27, 32, 44, 51, 62, 63]. In this study, we evaluated the AS of synaptic-related genes in *hSOD1*^{G93A} NPCs, under proliferating and differentiating conditions. Our results indicate that AS is deeply affected during NPCs differentiation, contributing to the functional defects observed in *hSOD1*^{G93A} progenitors.

To gain insight into AS deregulation in *hSOD1*^{G93A} NPCs we analyzed consensus motifs enriched within or nearby exons regulated during neuronal differentiation. Our analysis confirmed the important role of RBFOX1 and PTBP1 as regulators of the splicing program associated with neuronal differentiation and highlight other potential regulators of this switch, including RBM24 and SLM2. Notably, SLM2, encoded by the *Khdrbs3* gene, preferentially binds and regulates AS of transcripts encoding synaptic proteins and cell-type-specific loss-of-function studies uncovered the contribution of this RBP to hippocampal synapse specification [54, 55]. We also found that expression of RBFOX1 and PTBP1 is altered during neuronal differentiation of *hSOD1*^{G93A} NPCs.

PTBP1 and RBFOX proteins were shown to antagonistically govern the NPC-to-neuron transition by regulating neuron-specific exons [69]. Particularly, PTBP1 was shown to maintain apical progenitors, whereas RBFOX proteins promote neuronal differentiation [69]. Notably, *Rbfox1-/-* conditional knockout in mouse brain exhibited splicing changes in transcripts affecting synaptic function and neuronal excitation and showed upregulation of RBFOX2 protein as a compensatory mechanism [22]. Furthermore, *Rbfox* (1,2,3) triple knockout neurons exhibited defects in AS of many cytoskeletal, membrane, and synaptic proteins, and displayed immature electrophysiological activity, with severe perturbation of the axon initial segment, a subcellular structure important for action potential initiation [27]. On the other hand, homozygous mutation of *Ptbp1* led to embryonic lethality [47]. In line with these reports, our analysis of neuronal differentiation markers revealed a strong impairment of the differentiation program upon silencing of both *Ptbp1* and *Rbfox1*.

Collectively, our study indicates that the dynamic control of AS governing cell fate during cerebral cortical development is partially impaired in the *hSOD1*^{G93A} mouse model, contributing to the observed phenotype.

Conclusions

Our results reveal that the *hSOD1*^{G93A} mutation leads to significant changes in NPC properties, including clonogenicity and potential of differentiation, paralleled by changes in AS of synaptic-related genes. These changes are caused, at least in part, by the improper expression of splicing factors, including RBFOX1 and PTBP1.

Supplementary Information The online version contains supplementary material available at https://doi.org/10.1007/s00018-023-04893-7.

Acknowledgements The authors wish to thank Prof. Claudio Sette and Dr. Eleonora Cesari for technical support in NPCs experiments. The authors wish to thank Drs. Pierre de la Grange and Ariane Jolly (Genosplice, Paris) for the bioinformatic analysis.

Author contributions All the authors contributed to the study conception and design. Material preparation, data collection and analysis were performed by VV, VR, MG and GF. The first draft of the manuscript was written by VV and MPP. All the authors commented on previous versions of the manuscript. All the authors read and approved the final manuscript.

Funding This work was supported by grants from the Associazione Italiana Ricerca sul Cancro (AIRC) IG21877 to M.P.P., from Ministry of Health "Ricerca Corrente" to Fondazione Santa Lucia, RF-2019-12369105NR to A.F., and CNR IFT DBA.AD005.225 -NUTRAGE- FOE2021" to A.F.

Data availability The datasets analyzed during the current study are available in the GEO repository (GSE96950).

Declarations

Conflict of interest The authors have no relevant financial or non-financial interests to disclose.

Ethical approval All the animal procedures were approved by the Animal welfare office, Department of Public Health and Veterinary, Nutrition and Food Safety, General Management of Animal Care and Veterinary Drugs of the Italian Ministry of Health (protocol number 931/2017/PR) and carried out in agreement with European guidelines for the use of animals in research (2010/63/EU) and the requirements of Italian laws (D.L. 26/2014). Animals were kept in a virus/antigen-free facility with a light/dark cycle of 12 h at constant humidity and temperature and with food/water ad libitum.

References

1. Amendola J, Durand J (2008) Morphological differences between wild-type and transgenic superoxide dismutase 1 lumbar motoneurons in postnatal mice. J Comp Neurol 511:329–341. https://doi.org/10.1002/cne.21818
2. Atasoy D, Schoch S, Ho A, Nadasy KA, Liu X, Zhang W, Mukherjee K, Nosyreva ED, Fernandez-Chacon R, Missler M, Kavalali ET, Südhof TC (2007) Deletion of CASK in mice is lethal and impairs synaptic function. Proc Natl Acad Sci USA 104:2525–2530. https://doi.org/10.1073/pnas.0611003104
3. Avossa D, Grandolfo M, Mazzarol F, Zatta M, Ballerini L (2006) Early signs of motoneuron vulnerability in a disease model system: characterization of transverse slice cultures of spinal cord isolated from embryonic ALS mice. Neuroscience 138:1179–1194. https://doi.org/10.1016/j.neuroscience.2005.12.009
4. Baralle FE, Giudice J (2017) Alternative splicing as a regulator of development and tissue identity. Nat Rev Mol Cell Biol 18:437–451. https://doi.org/10.1038/nrm.2017.27
5. Barbosa-Morais NL, Irimia M, Pan Q, Xiong HY, Gueroussov S, Lee LJ, Slobodeniuc V, Kutter C, Watt S, Colak R, Kim T, Misquitta-Ali CM, Wilson MD, Kim PM, Odom DT, Frey BJ, Blencowe BJ (2012) The evolutionary landscape of alternative splicing in vertebrate species. Science 338:1587–1593. https://doi.org/10.1126/science.1230612
6. Bjornsson CS, Apostolopoulou M, Tian Y, Temple S (2015) It takes a village: constructing the neurogenic niche. Dev Cell 32:435–446. https://doi.org/10.1016/j.devcel.2015.01.010
7. Black DL, Grabowski PJ (2003) Alternative pre-mRNA splicing and neuronal function. Prog Mol Subcell Biol 31:187–216. https://doi.org/10.1007/978-3-662-09728-1_7
8. Bland CS, Wang ET, Vu A, David MP, Castle JC, Johnson JM, Burge CB, Cooper TA (2010) Global regulation of alternative splicing during myogenic differentiation. Nucleic Acids Res 38:7651–7664. https://doi.org/10.1093/nar/gkq614
9. Branchereau P, Martin E, Allain AE, Cazenave W, Supiot L, Hodeib F, Laupénie A, Dalvi U, Zhu H, Cattaert D (2019) Relaxation of synaptic inhibitory events as a compensatory mechanism in fetal SOD spinal motor networks. Elife. https://doi.org/10.7554/eLife.51402
10. Burgaya F, Toutant M, Studler JM, Costa A, Le Bert M, Gelman M, Girault JA (1997) Alternatively spliced focal adhesion kinase in rat brain with increased autophosphorylation activity. J Biol Chem 272:28720–28725. https://doi.org/10.1074/jbc.272.45.28720
11. Calarco JA, Zhen M, Blencowe BJ (2011) Networking in a global world: establishing functional connections between neural splicing regulators and their target transcripts. RNA 17:775–791. https://doi.org/10.1261/rna.2603911
12. Cashman NR, Durham HD, Blusztajn JK, Oda K, Tabira T, Shaw IT, Dahrouge S, Antel JP (1992) Neuroblastoma x spinal cord (NSC) hybrid cell lines resemble developing motor neurons. Dev Dyn 194:209–221. https://doi.org/10.1002/aja.1001940306
13. Chetkovich DM, Bunn RC, Kuo SH, Kawasaki Y, Kohwi M, Bredt DS (2002) Postsynaptic targeting of alternative postsynaptic density-95 isoforms by distinct mechanisms. J Neurosci 22:6415–6425. https://doi.org/10.1523/JNEUROSCI.22-15-06415.2002
14. Chuang M, Goncharov A, Wang S, Oegema K, Jin Y, Chisholm AD (2014) The microtubule minus-end-binding protein patronin/PTRN-1 is required for axon regeneration in C. elegans. Cell Rep 9:874–883. https://doi.org/10.1016/j.celrep.2014.09.054
15. de la Grange P, Dutertre M, Martin N, Auboeuf D (2005) FAST DB: a website resource for the study of the expression regulation of human gene products. Nucleic Acids Res 33:4276–4284. https://doi.org/10.1093/nar/gki738
16. Ferri A, Cozzolino M, Crosio C, Nencini M, Casciati A, Gralla EB, Rotilio G, Valentine JS, Carrì MT (2006) Familial ALS-superoxide dismutases associate with mitochondria and shift their redox potentials. Proc Natl Acad Sci USA 103:13860–13865. https://doi.org/10.1073/pnas.0605814103
17. Fidaleo M, Svetoni F, Volpe E, Miñana B, Caporossi D, Paronetto MP (2015) Genotoxic stress inhibits Ewing sarcoma cell growth by modulating alternative pre-mRNA processing of the RNA helicase DHX9. Oncotarget 6:31740–31757. https://doi.org/10.18632/oncotarget.5033
18. Filipchuk AA, Durand J (2012) Postnatal dendritic development in lumbar motoneurons in mutant superoxide dismutase 1 mouse model of amyotrophic lateral sclerosis. Neuroscience 209:144–154. https://doi.org/10.1016/j.neuroscience.2012.01.046
19. Fogarty MJ (2018) Driven to decay: excitability and synaptic abnormalities in amyotrophic lateral sclerosis. Brain Res Bull 140:318–333. https://doi.org/10.1016/j.brainresbull.2018.05.023
20. Fogarty MJ (2019) Amyotrophic lateral sclerosis as a synaptopathy. Neural Regen Res 14:189–192. https://doi.org/10.4103/1673-5374.244782
21. Furlanis E, Scheiffele P (2018) Regulation of neuronal differentiation, function, and plasticity by alternative splicing. Annu Rev Cell Dev Biol 34:451–469. https://doi.org/10.1146/annurev-cellbio-100617-062826
22. Gehman LT, Stoilov P, Maguire J, Damianov A, Lin CH, Shiue L, Ares M, Mody I, Black DL (2011) The splicing regulator Rbfox1 (A2BP1) controls neuronal excitation in the mammalian brain. Nat Genet 43:706–711. https://doi.org/10.1038/ng.841
23. Gupta S, Stamatoyannopoulos JA, Bailey TL, Noble WS (2007) Quantifying similarity between motifs. Genome Biol 8:R24. https://doi.org/10.1186/gb-2007-8-2-r24
24. Hardiman O, Al-Chalabi A, Chio A, Corr EM, Logroscino G, Robberecht W, Shaw PJ, Simmons Z, van den Berg LH (2017) Amyotrophic lateral sclerosis. Nat Rev Dis Primers 3:17085. https://doi.org/10.1038/nrdp.2017.85
25. Ip JY, Schmidt D, Pan Q, Ramani AK, Fraser AG, Odom DT, Blencowe BJ (2011) Global impact of RNA polymerase II

elongation inhibition on alternative splicing regulation. Genome Res 21:390–401. https://doi.org/10.1101/gr.111070.110
26. Irimia M, Blencowe BJ (2012) Alternative splicing: decoding an expansive regulatory layer. Curr Opin Cell Biol 24:323–332. https://doi.org/10.1016/j.ceb.2012.03.005
27. Jacko M, Weyn-Vanhentenryck SM, Smerdon JW, Yan R, Feng H, Williams DJ, Pai J, Xu K, Wichterle H, Zhang C (2018) Rbfox splicing factors promote neuronal maturation and axon initial segment assembly. Neuron 97:853-868.e856. https://doi.org/10.1016/j.neuron.2018.01.020
28. Kempermann G, Gage FH, Aigner L, Song H, Curtis MA, Thuret S, Kuhn HG, Jessberger S, Frankland PW, Cameron HA, Gould E, Hen R, Abrous DN, Toni N, Schinder AF, Zhao X, Lucassen PJ, Frisén J (2018) Human adult neurogenesis: evidence and remaining questions. Cell Stem Cell 23:25–30. https://doi.org/10.1016/j.stem.2018.04.004
29. Kuleshov MV, Jones MR, Rouillard AD, Fernandez NF, Duan Q, Wang Z, Koplev S, Jenkins SL, Jagodnik KM, Lachmann A, McDermott MG, Monteiro CD, Gundersen GW, Ma'ayan A (2016) Enrichr: a comprehensive gene set enrichment analysis web server 2016 update. Nucleic Acids Res 44:W90-97. https://doi.org/10.1093/nar/gkw377
30. Kuo JJ, Schonewille M, Siddique T, Schults AN, Fu R, Bär PR, Anelli R, Heckman CJ, Kroese AB (2004) Hyperexcitability of cultured spinal motoneurons from presymptomatic ALS mice. J Neurophysiol 91:571–575. https://doi.org/10.1152/jn.00665.2003
31. Leite SC, Sampaio P, Sousa VF, Nogueira-Rodrigues J, Pinto-Costa R, Peters LL, Brites P, Sousa MM (2016) The actin-binding protein α-adducin is required for maintaining axon diameter. Cell Rep 15:490–498. https://doi.org/10.1016/j.celrep.2016.03.047
32. Li Q, Zheng S, Han A, Lin CH, Stoilov P, Fu XD, Black DL (2014) The splicing regulator PTBP2 controls a program of embryonic splicing required for neuronal maturation. Elife 3:e01201. https://doi.org/10.7554/eLife.01201
33. Lin JW, Wyszynski M, Madhavan R, Sealock R, Kim JU, Sheng M (1998) Yotiao, a novel protein of neuromuscular junction and brain that interacts with specific splice variants of NMDA receptor subunit NR1. J Neurosci 18:2017–2027
34. Marcette JD, Chen JJ, Nonet ML (2014) The *Caenorhabditis elegans* microtubule minus-end binding homolog PTRN-1 stabilizes synapses and neurites. Elife 3:e01637. https://doi.org/10.7554/eLife.01637
35. Martynoga B, Drechsel D, Guillemot F (2012) Molecular control of neurogenesis: a view from the mammalian cerebral cortex. Cold Spring Harb Perspect Biol. https://doi.org/10.1101/cshperspect.a008359
36. Nilsen TW, Graveley BR (2010) Expansion of the eukaryotic proteome by alternative splicing. Nature 463:457–463. https://doi.org/10.1038/nature08909
37. Palombo R, Verdile V, Paronetto MP (2020) Poison-exon inclusion in DHX9 reduces its expression and sensitizes ewing sarcoma cells to chemotherapeutic treatment. Cells. https://doi.org/10.3390/cells9020328
38. Paridaen JT, Huttner WB (2014) Neurogenesis during development of the vertebrate central nervous system. EMBO Rep 15:351–364. https://doi.org/10.1002/embr.201438447
39. Pemberton K, Mersman B, Xu F (2018) Using ImageJ to assess neurite outgrowth in mammalian cell cultures: research data quantification exercises in undergraduate neuroscience lab. J Undergrad Neurosci Educ 16:A186–A194
40. Raj B, Blencowe BJ (2015) Alternative splicing in the mammalian nervous system: recent insights into mechanisms and functional roles. Neuron 87:14–27. https://doi.org/10.1016/j.neuron.2015.05.004
41. Ray D, Kazan H, Cook KB, Weirauch MT, Najafabadi HS, Li X, Gueroussov S, Albu M, Zheng H, Yang A, Na H, Irimia M, Matzat LH, Dale RK, Smith SA, Yarosh CA, Kelly SM, Nabet B, Mecenas D, Li W, Laishram RS, Qiao M, Lipshitz HD, Piano F, Corbett AH, Carstens RP, Frey BJ, Anderson RA, Lynch KW, Penalva LO, Lei EP, Fraser AG, Blencowe BJ, Morris QD, Hughes TR (2013) A compendium of RNA-binding motifs for decoding gene regulation. Nature 499:172–177. https://doi.org/10.1038/nature12311
42. Rezvykh AP, Ustyugov AA, Chaprov KD, Teterina EV, Nebogatikov VO, Spasskaya DS, Evgen'ev MB, Morozov AV, Funikov SY (2023) Cytoplasmic aggregation of mutant FUS causes multistep RNA splicing perturbations in the course of motor neuron pathology. Nucleic Acids Res. https://doi.org/10.1093/nar/gkad319
43. Rosen DR, Siddique T, Patterson D, Figlewicz DA, Sapp P, Hentati A, Donaldson D, Goto J, O'Regan JP, Deng HX (1993) Mutations in Cu/Zn superoxide dismutase gene are associated with familial amyotrophic lateral sclerosis. Nature 362:59–62. https://doi.org/10.1038/362059a0
44. Saito Y, Yuan Y, Zucker-Scharff I, Fak JJ, Jereb S, Tajima Y, Licatalosi DD, Darnell RB (2019) Differential NOVA2-mediated splicing in excitatory and inhibitory neurons regulates cortical development and cerebellar function. Neuron 101:707-720.e705. https://doi.org/10.1016/j.neuron.2018.12.019
45. Salomonis N, Schlieve CR, Pereira L, Wahlquist C, Colas A, Zambon AC, Vranizan K, Spindler MJ, Pico AR, Cline MS, Clark TA, Williams A, Blume JE, Samal E, Mercola M, Merrill BJ, Conklin BR (2010) Alternative splicing regulates mouse embryonic stem cell pluripotency and differentiation. Proc Natl Acad Sci USA 107:10514–10519. https://doi.org/10.1073/pnas.0912260107
46. Schlaepfer DD, Jones KC, Hunter T (1998) Multiple Grb2-mediated integrin-stimulated signaling pathways to ERK2/mitogen-activated protein kinase: summation of both c-Src- and focal adhesion kinase-initiated tyrosine phosphorylation events. Mol Cell Biol 18:2571–2585. https://doi.org/10.1128/MCB.18.5.2571
47. Shibayama M, Ohno S, Osaka T, Sakamoto R, Tokunaga A, Nakatake Y, Sato M, Yoshida N (2009) Polypyrimidine tract-binding protein is essential for early mouse development and embryonic stem cell proliferation. FEBS J 276:6658–6668. https://doi.org/10.1111/j.1742-4658.2009.07380.x
48. Suzuki H, Osaki K, Sano K, Alam AH, Nakamura Y, Ishigaki Y, Kawahara K, Tsukahara T (2011) Comprehensive analysis of alternative splicing and functionality in neuronal differentiation of P19 cells. PLoS ONE 6:e16880. https://doi.org/10.1371/journal.pone.0016880
49. Taverna E, Götz M, Huttner WB (2014) The cell biology of neurogenesis: toward an understanding of the development and evolution of the neocortex. Annu Rev Cell Dev Biol 30:465–502. https://doi.org/10.1146/annurev-cellbio-101011-155801
50. Taylor JP, Brown RH, Cleveland DW (2016) Decoding ALS: from genes to mechanism. Nature 539:197–206. https://doi.org/10.1038/nature20413
51. Torres-Méndez A, Pop S, Bonnal S, Almudi I, Avola A, Roberts RJV, Paolantoni C, Alcaina-Caro A, Martín-Anduaga A, Haussmann IU, Morin V, Casares F, Soller M, Kadener S, Roignant JY, Prieto-Godino L, Irimia M (2022) Parallel evolution of a splicing program controlling neuronal excitability in flies and mammals. Sci Adv 8:eabk0445. https://doi.org/10.1126/sciadv.abk0445
52. Toutant M, Studler JM, Burgaya F, Costa A, Ezan P, Gelman M, Girault JA (2000) Autophosphorylation of Tyr397 and its phosphorylation by Src-family kinases are altered in focal-adhesion-kinase neuronal isoforms. Biochem J 348(Pt 1):119–128
53. Traiffort E, Morisset-Lopez S, Moussaed M, Zahaf A (2021) Defective oligodendroglial lineage and demyelination in amyotrophic lateral sclerosis. Int J Mol Sci. https://doi.org/10.3390/ijms22073426
54. Traunmüller L, Gomez AM, Nguyen TM, Scheiffele P (2016) Control of neuronal synapse specification by a highly dedicated

alternative splicing program. Science 352:982–986. https://doi.org/10.1126/science.aaf2397
55. Traunmüller L, Schulz J, Ortiz R, Feng H, Furlanis E, Gomez AM, Schreiner D, Bischofberger J, Zhang C, Scheiffele P (2023) A cell-type-specific alternative splicing regulator shapes synapse properties in a trans-synaptic manner. Cell Rep 42:112173. https://doi.org/10.1016/j.celrep.2023.112173
56. Trias E, Ibarburu S, Barreto-Núñez R, Barbeito L (2017) Significance of aberrant glial cell phenotypes in pathophysiology of amyotrophic lateral sclerosis. Neurosci Lett 636:27–31. https://doi.org/10.1016/j.neulet.2016.07.052
57. Ule J, Blencowe BJ (2019) Alternative splicing regulatory networks: functions, mechanisms, and evolution. Mol Cell 76:329–345. https://doi.org/10.1016/j.molcel.2019.09.017
58. Ule J, Stefani G, Mele A, Ruggiu M, Wang X, Taneri B, Gaasterland T, Blencowe BJ, Darnell RB (2006) An RNA map predicting Nova-dependent splicing regulation. Nature 444:580–586. https://doi.org/10.1038/nature05304
59. van Zundert B, Peuscher MH, Hynynen M, Chen A, Neve RL, Brown RH, Constantine-Paton M, Bellingham MC (2008) Neonatal neuronal circuitry shows hyperexcitable disturbance in a mouse model of the adult-onset neurodegenerative disease amyotrophic lateral sclerosis. J Neurosci 28:10864–10874. https://doi.org/10.1523/JNEUROSCI.1340-08.2008
60. Verdile V, Guizzo G, Ferrante G, Paronetto MP (2021) RNA targeting in inherited neuromuscular disorders: novel therapeutic strategies to counteract mis-splicing. Cells. https://doi.org/10.3390/cells10112850
61. Verdile V, Svetoni F, La Rosa P, Ferrante G, Cesari E, Sette C, Paronetto MP (2022) EWS splicing regulation contributes to balancing Foxp1 isoforms required for neuronal differentiation. Nucleic Acids Res 50:3362–3378. https://doi.org/10.1093/nar/gkac154
62. Vuong CK, Black DL, Zheng S (2016) The neurogenetics of alternative splicing. Nat Rev Neurosci 17:265–281. https://doi.org/10.1038/nrn.2016.27
63. Wamsley B, Jaglin XH, Favuzzi E, Quattrocolo G, Nigro MJ, Yusuf N, Khodadadi-Jamayran A, Rudy B, Fishell G (2018) Rbfox1 mediates cell-type-specific splicing in cortical interneurons. Neuron 100:846-859.e847. https://doi.org/10.1016/j.neuron.2018.09.026
64. Wang ET, Sandberg R, Luo S, Khrebtukova I, Zhang L, Mayr C, Kingsmore SF, Schroth GP, Burge CB (2008) Alternative isoform regulation in human tissue transcriptomes. Nature 456:470–476. https://doi.org/10.1038/nature07509
65. Weyn-Vanhentenryck SM, Feng H, Ustianenko D, Duffié R, Yan Q, Jacko M, Martinez JC, Goodwin M, Zhang X, Hengst U, Lomvardas S, Swanson MS, Zhang C (2018) Precise temporal regulation of alternative splicing during neural development. Nat Commun 9:2189. https://doi.org/10.1038/s41467-018-04559-0
66. Xu K, Zhong G, Zhuang X (2013) Actin, spectrin, and associated proteins form a periodic cytoskeletal structure in axons. Science 339:452–456. https://doi.org/10.1126/science.1232251
67. Yamashita S, Ando Y (2015) Genotype-phenotype relationship in hereditary amyotrophic lateral sclerosis. Transl Neurodegener 4:13. https://doi.org/10.1186/s40035-015-0036-y
68. Yeo GW, Xu X, Liang TY, Muotri AR, Carson CT, Coufal NG, Gage FH (2007) Alternative splicing events identified in human embryonic stem cells and neural progenitors. PLoS Comput Biol 3:1951–1967. https://doi.org/10.1371/journal.pcbi.0030196
69. Zhang X, Chen MH, Wu X, Kodani A, Fan J, Doan R, Ozawa M, Ma J, Yoshida N, Reiter JF, Black DL, Kharchenko PV, Sharp PA, Walsh CA (2016) Cell-type-specific alternative splicing governs cell fate in the developing cerebral cortex. Cell 166:1147-1162.e1115. https://doi.org/10.1016/j.cell.2016.07.025
70. Zou ZY, Zhou ZR, Che CH, Liu CY, He RL, Huang HP (2017) Genetic epidemiology of amyotrophic lateral sclerosis: a systematic review and meta-analysis. J Neurol Neurosurg Psychiatry 88:540–549. https://doi.org/10.1136/jnnp-2016-315018
71. Šušnjar U, Škrabar N, Brown AL, Abbassi Y, Phatnani H, Cortese A, Cereda C, Bugiardini E, Cardani R, Meola G, Ripolone M, Moggio M, Romano M, Secrier M, Fratta P, Buratti E, Consortium NA (2022) Cell environment shapes TDP-43 function with implications in neuronal and muscle disease. Commun Biol 5:314. https://doi.org/10.1038/s42003-022-03253-8